

Synthesis and Characterization of Pure and Alkali Catalysts Metals-Doped Tin Dioxide

Hadj Benhebal and Messaoud Chaib

Laboratoire de Chimie et Environnement, Université de Tiaret,
BP 78 Zaaroura, Tiaret 14000, Algeria

Abstract: In order to improve the photocatalytic properties of tin dioxide, nanosized powders of SnO₂ photocatalysts doped by alkali metals (Li, Na and K) were synthesized by sol-gel process. The physical properties of these materials were characterized by X-ray diffraction, nitrogen adsorption-desorption, Scanning Electron Microscopy and Ultraviolet-visible diffuse reflectance spectroscopy. The photocatalytic tests under UV radiation conducted on four aromatic compounds (phenol, paranitrophenol, pentachlorophenol and benzoic acid) showed that tin dioxide doped with sodium possesses the highest photocatalytic activity; The Li-doped SnO₂ is moderately active, while K-doped catalyst measured the smallest activity.

Key words: Tin dioxide · Sol-gel · Alkali metals · Photocatalysis · Aromatic compounds

INTRODUCTION

In recent decades, a large number of applications associated with the photocatalysis have seen the day in areas such as clean water or air, hydrogen production or self-cleaning materials. This method has been suggested in environmental protection due to its ability to oxidize the organic and inorganic substances [1].

Semiconductors metal such as ZnO, TiO₂ and SnO₂ have been recognized to be preferable materials for photocatalytic processes due to their high photo-sensitivity, non-toxic nature, low cost and chemical stability [2, 3]. However, the band gap width of TiO₂ (3.2 eV), ZnO (3.3 eV) and SnO₂ (3.6 eV) limits the absorption ability of the high-energy portion (UV) of the sunlight, which results in the relatively small efficiency [4].

Tin dioxide (SnO₂) is an important semiconducting material which has been widely used in an extensive range of applications such as catalysts [5, 6], gas sensors [7, 8], heat mirrors [9, 10], varistors [11, 12] and transparent electrodes for solar cells [13, 14], glass melting electrodes and optoelectronic devices [15].

Recent research work has been devoted for the development of synthesis of SnO₂ nanoparticles of varying sizes in a controllable manner [16], among the different routes such as sol-gel process, precipitation, hydrothermal, solvothermal, etc. Sol-gel process is an

effective method preferred to control the textural and surface properties of metal oxides. This method is based on the hydrolysis and polycondensation of a metal salt, which ultimately yields hydroxide or oxide under certain conditions [17] and provides a facilitated route to prepare uniform, well dispersed and well-crystallized SnO₂ nanoparticles.

Doping has been widely used to alter the properties of nanocrystallized solids in desirable and controllable ways [18, 19]. Dopants can strongly influence electronic behaviour of bulk semiconductors. Doped tin dioxide nanocrystals have been studied in recent years [20, 21].

The first aim of this work is to synthesize a crystallized pure and alkali metals doped- SnO₂ powders by sol-gel process. Photocatalyst powders are characterized by using X-Ray diffraction (XRD), Scanning electron microscopy (SEM), Nitrogen adsorption isotherms and UV-Vis spectroscopy. The second aim of this work is to study the photocatalytic activity of different photocatalysts under UV radiation.

Experimental Section

Photocatalysts Preparation: The photocatalysts were prepared at the base of the tin dioxide doped by alkali metals (Lithium, Sodium and Potassium) with a dopant concentration of 10 wt. % using the sol-gel process, according to the following protocol:

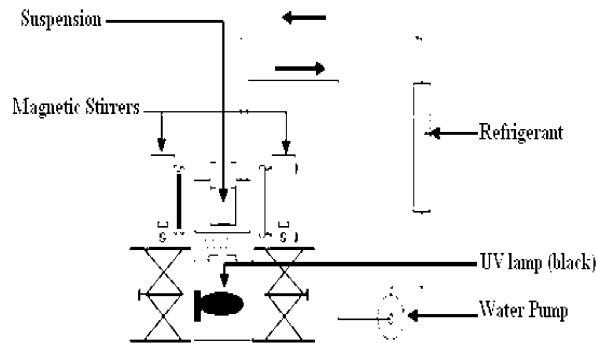


Fig. 1: Reactor used in the photocatalytic experiments

37 mmol of SnCl_2 (Aldrich, Purity: 99.99%) was mixed in 100 mL of absolute ethanol (Merck, Purity: 99.9%) under stirring and refluxing at 80°C under nitrogen ambient in a closed vessel for 2 h. A white tin alkoxide powder was obtained after heating of solution at 80°C under vacuum condition [22], to which 50 mL of absolute ethanol and 50 mL of LiNO_3 (Tucker-USA, 99.5%), NaNO_3 (Cheminova: International S.A, 99.5%) or KNO_3 (BIOCHEM, Chemopharma, 99.9%), solution with respective concentrations $1.85 \text{ mmol. L}^{-1}$, $1.83 \text{ mmol. L}^{-1}$ and $1.85 \text{ mmol. L}^{-1}$ were added. This solution was then stirred and heated for 2 h at 50°C .

The stirring was stopped and gelation underwent in about 5 days. Afterwards, the gel was dried at 110°C for 2h. Finally, the powder was calcined under flowing air (0.1 mmol s^{-1}) at 700°C for 4 h.

Catalysts Characterization: To determine the crystalline phase and the crystallite size of the photocatalysts, powder X-ray diffractograms were recorded applying Philips PW 1830 diffractometer using the $\text{Cu-K}\alpha$ line ($\lambda=0.15458 \text{ nm}$). The phases present were identified by comparison with JCPDS cards and the crystallite sizes were calculated by X-ray line broadening profile analysis according to the Debye-Scherrer formula.

Morphology and particles sizes of photocatalysts were examined by SEM on a Jeol JSM-840 under high vacuum, at an acceleration voltage of 20 kV. The samples were deposited onto carbon tape and coated with gold in a Balzers plasma sputterer (30 s at 30 mA).

Specific surface areas (S_{BET}) of the samples were performed using the BET method, the nitrogen adsorption-desorption isotherms were measured at -196°C on a Fisons Sorptomatic 1990 after outgassing for 24 h at ambient temperature.

Ultraviolet-visible diffuse reflectance spectra (UV-Vis DRS) of the samples were measured on a Varian Cary 5000

UV/Vis/NIR spectrophotometer, equipped with a Varian External DRA-2500 integrating sphere, using BaSO_4 as the reference.

Photocatalytic Experiments: Four organic compounds (phenol, paranitrophenol, pentachlorophenol and benzoic acid) were chosen to evaluate the photocatalytic activity of synthesized photocatalysts. The study of degradation of the compounds in question was carried out at 20°C using a water-cooled cylindrical 200 mL glass reactor (Fig.1), with external lamp (125 W UV lamps, Black light Mercury HgV). The experimental conditions are fixed as: The amount of catalyst powder, [Photocatalyst], was kept at 1.0 g L^{-1} , the initial concentration of pollutant, C_0 , was 0.2 g L^{-1} and the pH of the solution was fixed to 6.5.

Before each photocatalytic test, the mixture was kept in the dark for 1h to ensure that the adsorption-desorption equilibrium was reached before illumination. The sample was then taken out at the end of the dark adsorption period, just before the light was turned on, in order to determine the pollutant concentration in solution.

When the lamp was turned on, the experiment started. After a given irradiation time, the sample was taken out from reactor, then the catalyst was removed by centrifugation and the remaining pollutant concentration in the solution was measured with the photocoulometric method of 4-amino-antipyrine [23]. Repetition tests were made to ensure the reproducibility of results. So all the photocatalytic result presented in this work are the mean of three replicates.

RESULTS AND DISCUSSION

Characterization of Synthesized Photocatalysts:

Fig. 2 shows the X-ray diffractograms of the undoped and (Li, Na and K) doped SnO_2 powders heated at 700°C for 4hours. For all samples, the peak position agree well with the reflection of tetragonal rutile structure ($a= b= 0.4731 \text{ nm}$ and $c = 0.3173 \text{ nm}$) of pure SnO_2 (JCPDS Card N° 88-2348) and the diffraction peaks arise at (110), (101), (200), (111), (211), (220) and (002) without any other phases detected, indicating that all ions of alkali metals were embedded into the crystal lattice of SnO_2 . The peaks appear more intense in the case of doped powders which may indicate a relatively high degree of crystallinity. A decrease in crystallinity is observed from lithium to potassium (Fig. 2). The average size of crystallites for the different photocatalysts is calculated from profile Scherrer's formula based on line broadening analysis [24]. And their values are cited in Table 1.

Table 1: Characteristics of the different SnO₂ photocatalysts synthesized.

Sample	Size(nm)	Surface area(m ² /g)	λ(nm)	E _g (eV)
Undoped SnO ₂	36	25,0	342	3.625
Li-doped SnO ₂	14	23.8	382	3.246
Na-doped SnO ₂	12.5	28.6	398	3.115
K-doped SnO ₂	7.5	22.3	422	2.938

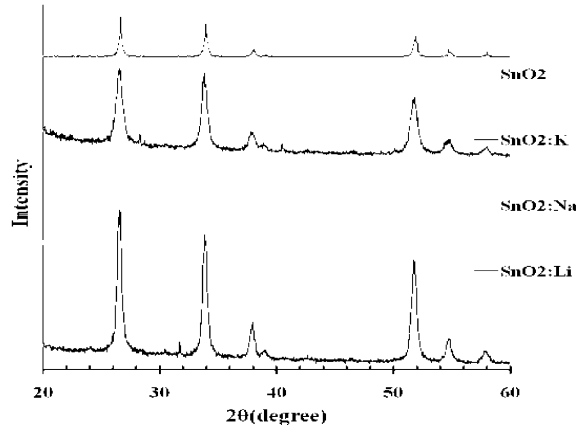


Fig. 2: XRD patterns of undoped and doped SnO₂ powders.

By SEM analysis, it is observed in Fig.3b-d that the calcined powders of SnO₂ doped by alkali metals (Li, Na and K) are composed of agglomerates; these clusters are composed of aggregates of heterogeneous sizes in the case of Li-doped SnO₂ and homogeneous sizes in the case of K-doped SnO₂. The agglomerates formed the powders

of Na-doped SnO₂ are much more orderly and composed of particles with sizes relatively homogeneous. The mean size of SnO₂ particles is equal to 50 nm (Fig. 3a) which is near from the values calculated by XRD.

A nitrogen adsorption-desorption isotherm was carried out to analyze the textural properties of pure and doped SnO₂ powders and it is presented in Fig. 4a-d. This isotherm displays a slight increase of the adsorbed volume at very small p/p_0 values, which is characteristic of the presence of micropores (< 2 nm) inside SnO₂ particles [25]. Furthermore, the isotherm shows a hysteresis at p/p_0 from 0.4 to 1, due to capillary condensation in mesopores (2-50 nm) corresponding in the voids between the 30-50 nm SnO₂ powder particles [25]. Finally, Table.1 provides the values of specific surface area obtained by the BET method [25] of the pure and doped SnO₂ powders.

UV-Visible absorption spectra are a particularly suitable technique to diagnose the band structure in the materials [26]. Fig. 5 shows the UV-visible (UV-vis) diffuse reflectance spectra of undoped and Li, Na and K-doped SnO₂. Using the method reported by Provenzano *et al.* [27] and the simplified form of energy-wavelength relationship, E_g (eV) = 1240/λ [28, 29], the absorption edge and band gap width values of different photocatalysts were calculated and are reported in Table.1. From these results, it was noticed that doping with alkali metals decreased the energy band gap (E_g) of SnO₂.

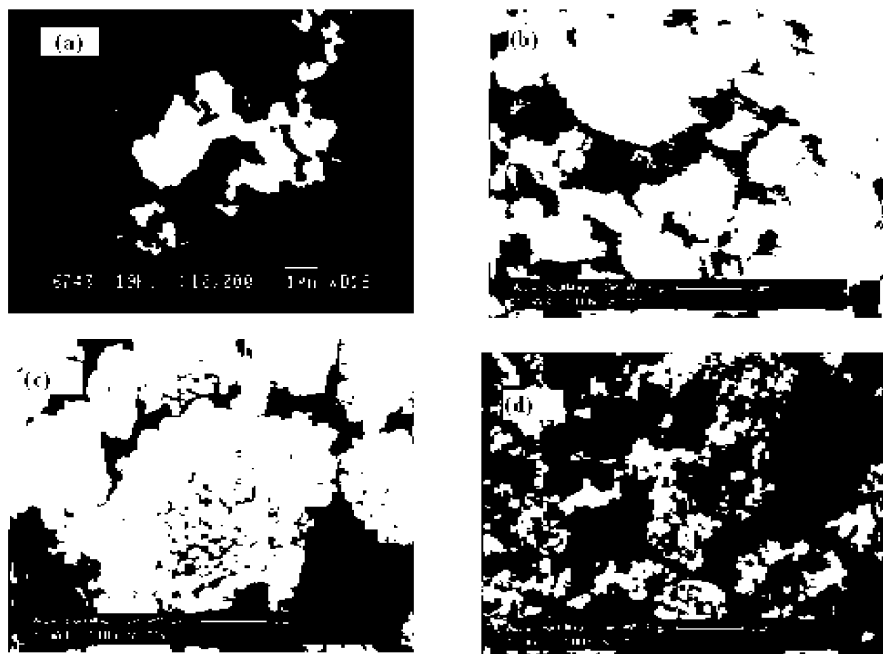


Fig. 3: SEM images of: (a) Undoped SnO₂, (b) Li-doped SnO₂, (c) Na-doped SnO₂ and (d) K-doped SnO₂.

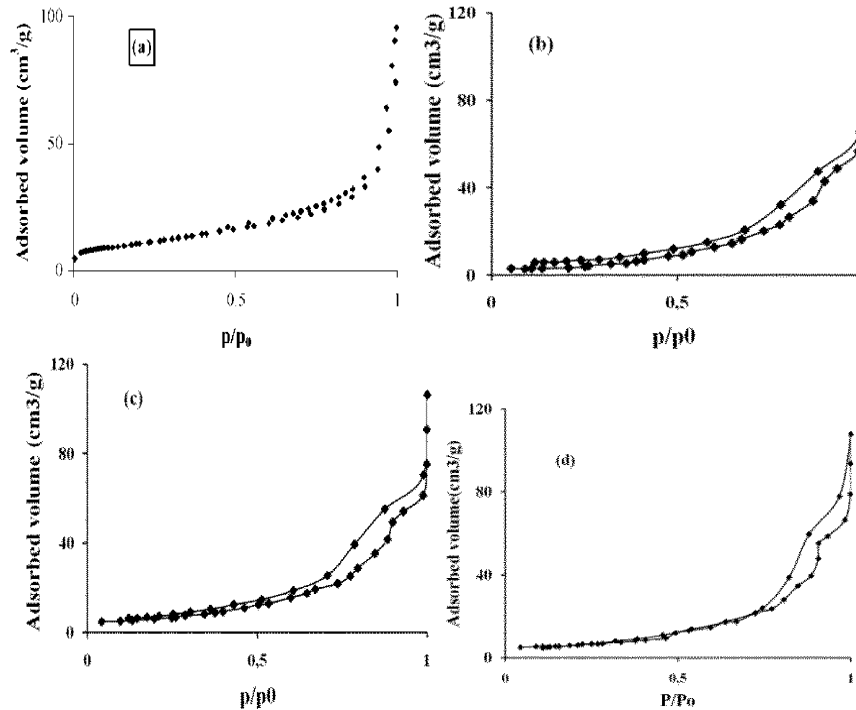


Fig. 4: N₂ adsorption/desorption isotherms for undoped and doped SnO₂: (a) Undoped-SnO₂, (b) Li-doped SnO₂, (c) Na-doped SnO₂ and (d) K-doped SnO₂.

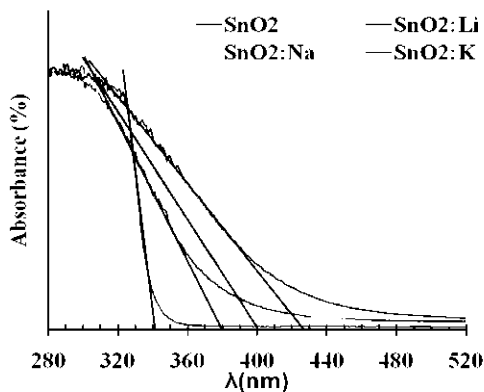


Fig. 5: UV-Vis spectra of undoped and doped SnO₂.

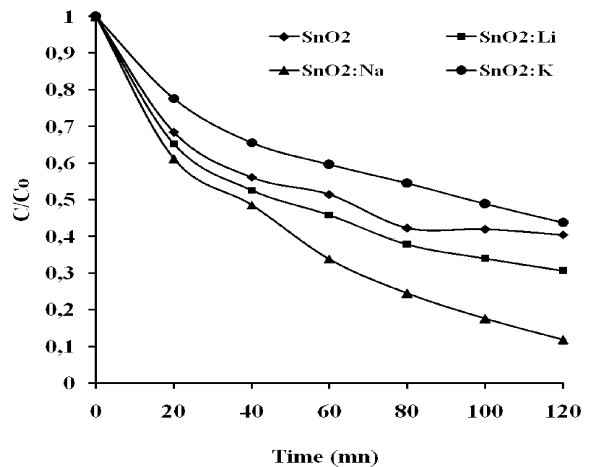


Fig. 6: Degradation of phenol as a function of time, where C₀ is the initial phenol concentration (g L⁻¹) and C is the phenol concentration at the time t. C₀ = 0.2 g L⁻¹, [photocatalyst] = 1.0 g L⁻¹, pH = 6.5 and irradiation time = 120 mn.

Photocatalytic Activity of Pure and Doped-SnO₂ Powder: Fig 6-9 shows respectively, the photocatalytic degradation of phenol, paranitrophenol, pentachlorophenol and benzoic acid in contact with different photocatalysts powder as a function of time at pH 6.5 and T=20°C.

It is observed that the Na doped SnO₂ has the largest photocatalytic activity compared to other photocatalysts and for virtually all organic compounds studied, it achieves a degradation of about 88.2% for the phenol solution, 68.55% for the paranitrophenol solution, 76.24%

for the pentachlorophenol solution and 62.25% for the benzoic acid solution after 2 hours of irradiation. This finding could be discussed in terms of the role of Na dopant in the crystallite size of SnO₂ from 36 to 12.5 nm and increasing its S_{BET} from 25 to 28.6 m²/g. Research has

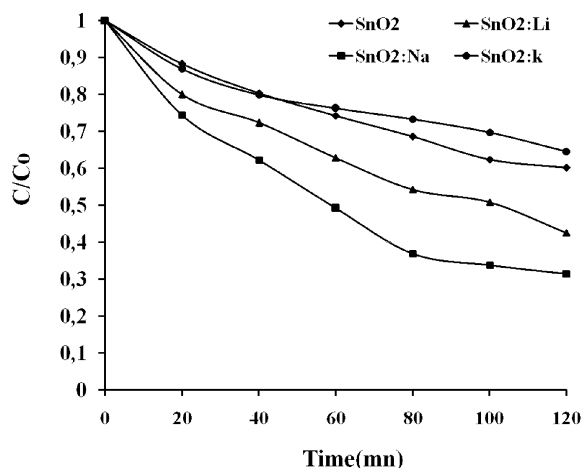


Fig. 7: Degradation of paranitrophenol as a function of time, where C_0 is the initial paranitrophenol concentration (g L^{-1}) and C is the paranitrophenol concentration at the time t . $C_0 = 0.2 \text{ g L}^{-1}$, [photocatalyst] = 1.0 g L^{-1} . pH = 6.5 and irradiation time = 120 mn.

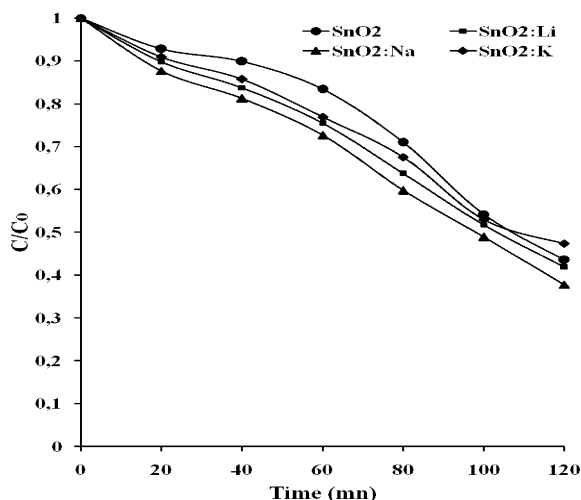


Fig. 9: Degradation of benzoic acid as a function of time, where C_0 is the initial benzoic acid concentration (g L^{-1}) and C is the benzoic acid concentration at the time t . $C_0 = 0.2 \text{ g L}^{-1}$, [photocatalyst] = 1.0 g L^{-1} . pH = 6.5 and irradiation time = 120 mn.

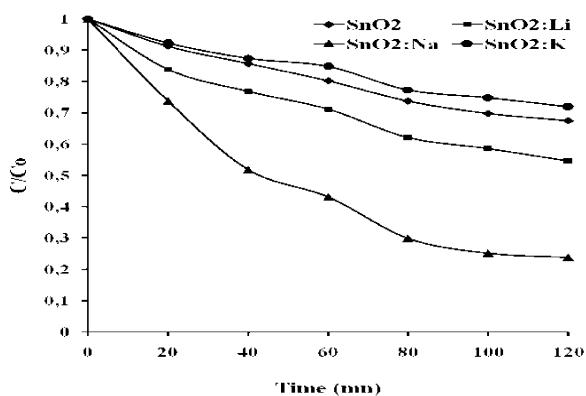


Fig. 8: Degradation of pentachlorophenol as a function of time, where C_0 is the initial pentachlorophenol concentration (g L^{-1}) and C is the pentachlorophenol concentration at the time t . $C_0 = 0.2 \text{ g L}^{-1}$, [photocatalyst] = 1.0 g L^{-1} . pH = 6.5 and irradiation time = 120 mn.

shown that the particle size plays on two important characteristics of the photocatalyst: Its surface area and its dispersion in solution. Reduce the small particle size increases the contact area and improves the dispersion of the powder in solution thus promoting interactions photons/catalyst/pollutant [30-32].

A lesser extent, we can observe that doping by lithium could improve the photocatalytic activity of tin dioxide since the degradation rates obtained with Li-doped SnO_2 are much higher than those obtained with undoped SnO_2 .

On the other hand, the results represented in Figs 6-9, show that the effect of doping by potassium on the photocatalytic properties is negative. This effect is translated by an effective decrease in rates of degradation compared to those recorded for pure SnO_2 catalyst. In light of the smallest crystallite of SnO_2 due doping with K, this particular catalyst should exhibit the highest activity and not the smallest activity. This discrepancy could be resolved by considering the optical properties of K-doped SnO_2 whose E_g value measures the smallest value (2.938), making a photocatalyst active under visible light and less active under irradiation SnO_2 UV.

CONCLUSION

The synthesis and doping of SnO_2 by alkali metals (Li, Na and K) were performed using the sol-gel process.

The characterization of these materials showed that doping of tin dioxide by these elements allows obtaining powders of small size with a slight increase in surface area of Na-doped SnO_2 .

Photocatalytic degradation of four organic compounds chosen in this study shows that doping by alkali metals (Li, Na and k) caused two different effects on the photocatalytic properties of tin dioxide. A positive effect was recorded in the case of doping with lithium and sodium. The negative effect was observed in the case of tin dioxide doped by potassium.

This study has enabled us to highlight the qualities photocatalytic of Na-doped SnO₂ with can be improved by varying the doping level or change the method of synthesis.

ACKNOWLEDGEMENTS

The authors would like to thank to all research teams of laboratory of chemical Engineering, Department of applied chemistry, University of liege for the different characterization and for their support.

REFERENCES

1. Fox, M.A. and M.T. Dulay, 1993. Heterogeneous photocatalysis. *Chemical Rev.*, 93: 341-357.
2. Lakshmi, B.B., C.J. Patrissi and C.R. Martin, 1997. *Chem. Mater.*, 9: 2544-2550.
3. Hara, K., T. Horiguchi and T. Kinoshita, 2000. *Sol. Energy Mater. Sol. Cell.* 64: 115-134.
4. Coey, J.M.D., M. Venkatesan and C.B. Fitzgerald, 2005. *Nat. Mater.*, 4: 173-179.
5. Chou, L., Y. Cai, B. Zhang, J. Niu, S. Ji and S. Li, 2003. Influence of SnO₂-doped W- Mn/SiO₂ for oxidative conversion of methane to high hydrocarbons at elevated pressure, *Appl. Catal. A: Gen.*, 238: 185-191.
6. Wierzchowski, P.T. and L.W. Zatorski, 2003. Kinetics of catalytic oxidation of carbonmonoxide and methane combustion over alumina supported Ga₂O₃, SnO₂ or V₂O₅, *Appl. Catal. B: Environ.* 1352: 1-13.
7. Moulson, A.J. and J.M. Herbert, 1990. *Electroceraamics*, Chapman and Hall, New York, 1990.
8. Shimizu, Y. and M. Egashira, 1999. Basic aspects and challenges of semiconductor gas sensors, *MRS Bull.*, 24(6): 18-24.
9. Kojima, M., F. Takahashi, K. Kinoshita and T. Nishibe, Ichidate M transparent furnace made of heat mirror, *Thin Solid Films.* 392: 349-354.
10. Lampert, C.M., 1981. Heat mirror coatings for energy conserving windows, *Solar Energy Mater.*, 6(1): 1-41.
11. Wang, J.F., Y.J. Wang, W.B. Su, H.C. Chen and W.X. Wang, 2002. Novel (Zn, Nb)-doped SnO₂ varistors, *Mater. Sci. Eng.*, B96: 8-13.
12. Santos, M.R.C., P.R. Bueno, E. Longo and J.A. Varela, 2001. Effect of oxidizing and reducing atmospheres on the electrical properties of dense SnO₂ based varistors, *J. Eur. Ceram. Soc.*, 21(2): 161-167.
13. Moustafid, T.E., H. Cachet, B. Tribollet and D. Festy, 2002. Modified transparent SnO₂ electrodes as efficient and stable cathodes for oxygen reduction, *Electrochim. Acta.* 47(8): 1209-1215.
14. Okuya, M., S. Kaneko, K. Hiroshima, I. Yaggi and K. Murakami, 2001. Low temperature deposition of SnO₂ thin films as transparent electrodes by spray pyrolysis of tetra-n-butyltin (IV), *J. Eur. Ceram. Soc.*, 21(10-11): 2099-2102.
15. Kim, T.W., D.U. Lee, D.C. Choo, J.H. Kim, H.J. Kim, J.H. Jeong, M. Jung, J.H. Bahang, H.L. Park, Y.S. Yoon and J.Y. Kim, 2002. Optical parameters in SnO₂ nanocrystalline textured films grown on p-InSb (111) substrates, *J. Phys. Chem. Solids.* 63: 881-885.
16. Sathyaseelan B., *et al.* / 2010. *Materials Chemistry and Physics.* 124: 1046-1050.
17. Chandra A., P. Bose and Thangadurai, S. Ramasamy, 2006. *Mater. Chem. Phys.*, 95: 72.
18. Norris, D.J., A.L. Efros and S.C. Erwin, 2008. *Sci.*, 319: 1776.
19. Pradhan, N., D. Goorskey, J. Thessing and X.G. Peng, 2005. *J. Am. Chem. Soc.*, 127: 7586.
20. Sadeh, A., S. Sladkevich, F. Gelman, P. Prihodchenko, I. Baumberg, O. Berezin and O. Lev, 2007. *Anal. Chem.*, 79: 5188.
21. Giannakopoulou, T., N. Todorova, C. Trapalis and T. Vaimakis, 2007. *Mater. Lett.*, 61: 4474.
22. Novinrooz, A. and P. Sarabadani, 2006. *J. Garousi, Iran. J. Chem. Chem. Eng.*, 25: 31.
23. Clesceri, E.A. and A. Greenberg, 1995. *Standard Methods for Examination of Water and Wastewater*, 19th ed. APHA, AWWA and WEF, Washington, DC, 1995., analyzed with a 1201 Shimadzu Spectrophotometer.
24. Bergeret, G., P. Gallezot, in: G. Ertl, H. Knözinger and J. Weitkamp (Eds.), 1997. *Handbook of Heterogeneous Catalysis*, Wiley-VCH, Weinheim, pp: 439.
25. Lecloux, A.J., 1989. In: Anderson J.R. and M. Boudart (Eds.), *Catalysis: Science and Technology*, Springer, Berlin, 2: 171.
26. He, Z., *et al.* / 2011. *J. Hazardous Materials.*
27. Provenzano, P.L., G.R. Jindal, J.R. Sweet, W.B. White and J. Luminescence, 2001. 92: 297.
28. Feng, J., J. Han and X. Zhao, 2009. Synthesis of CuInS₂ quantum dots on TiO₂ porous films by solvothermal method for absorption layer of solar cells. *Progress in Organic Coatings*, 64: 268-273.

29. Anbuchudar Azhagan and Ganesan/Rec Res. Sci. Tech., 2010. 2: 107.
30. Fallet, M., S. Permpoon, J.L. Deschanvres and M. Langlet, 2006. *J. Mater. Sci.*, 41(10): 2915.
31. Zhang, Z.C., C. Wang. R. Zakaria and J.Y. Ying, 1998. *J. Phys. Chem. B.*, 102(52): 10871.
32. Maira, A.J., K.L. Yeung, C.Y. Lee. P.L. Yue and C.K. Chan, 2000. *J. Catal.*, 192(1): 185.